Sensors and Materials, Vol. 35, No. 9 (2023) 3201–3209
MYU Tokyo

S & M 3385

Amino-functionalized Cup-stacked Carbon Nanofibers as Electrode Materials for Suppressing Protein Fouling

Yuka Ashitani,[1] Kazutake Takada,[2] and Kikuo Komori[1,3*]

[1]Graduate School of System Engineering, Kindai University,
Takaya-Umenobe, Higashi-Hiroshima, Hiroshima 739-2116, Japan
[2]Graduate School of Engineering, Nagoya Institute of Technology,
Gokiso, Showa, Nagoya 466-8555, Japan
[3]Department of Biotechnology and Chemistry, Kindai University,
Takaya-Umenobe, Higashi-Hiroshima, Hiroshima 739-2116, Japan

(Received July 13, 2023; accepted September 22, 2023)

Keywords: carbon nanomaterials, graphene edges, electrochemical sensing, electron transfer rate constant

Amino-functionalized cup-stacked carbon nanofibers (CSCNFs), the surface of which provides highly ordered graphene edges and amino groups, were investigated as electrode materials by using typical redox species in electrochemistry, namely, $[Fe(CN)_6]^{3-/4-}$ and $Fe^{2+/3+}$. The electron transfer rate of $[Fe(CN)_6]^{3-/4-}$ was accelerated and that of $Fe^{2+/3+}$ was decelerated by amino groups, mainly owing to the electrostatic interaction and repulsion, respectively. The hydrophilic amino-functionalized CSCNF surface also allowed the suppression of protein adsorption. Thus, the amino-functionalized CSCNFs would be useful electrode materials for biosensing and other electrochemical devices.

1. Introduction

Carbon nanomaterials including single-walled carbon nanotubes, graphene flakes, and graphite nanofibers are one of the outstanding and promising electrode materials for batteries, fuel cells, and electrochemical sensors because of their large specific surface area and high electrical conductivity. In particular, graphene edges are known to often exhibit unique electronic, chemical, and magnetic properties.(1) In the electrochemistry field, the edge-orientated pyrolytic graphite surface is widely known to be more electroactive than the basal plane pyrolytic graphite surface.(2) This phenomenon is also considered to be akin to stacked graphene nanofibers, such as platelet carbon nanofibers, herringbone carbon nanofibers, and cup-stacked carbon nanofibers (CSCNFs), which provide a high density of exposed and reactive graphene edges at fiber surfaces.(3,4) Hence, the stacked graphene nanofibers are suitable for constructing highly electroactive three-dimensional electrode networks.

Recently, we have reported that the CSCNFs worked as an electric nanowire and an enzyme support for electrochemical biosensors.(5,6) In addition, oxygenated CSCNFs, at the surface of

*Corresponding author: e-mail: komori@hiro.kindai.ac.jp
https://doi.org/10.18494/SAM4577

ISSN 0914-4935
https://myukk.org/

which negatively charged oxygen-containing functional groups are introduced by oxygenation, allowed the tuning of sensitivities and selectivities to redox species.[7,8] If positively charged functional groups, such as amino groups, are introduced to the CSCNF surface, the sensitivities and selectivities to redox species should also be tunable and different from those for the oxygenated CSCNF electrode. However, the electrochemical properties of amino-functionalized CSCNFs (NH_2-CSCNFs) have not yet been well investigated to the best of our knowledge.

To functionalize the surface of the carbon electrode, plasma treatment methods are often employed, but special apparatuses are used for the synthesis of nitrogen-doped carbon.[9,10] We previously treated the surfaces of graphite nanofibers using a general air plasma apparatus. Although air plasma is associated with oxygen and nitrogen gases, oxygen atoms were almost doped to the graphite nanofiber surface[11] probably owing to the reaction with oxygen or ambient moisture. On the other hand, amino-functional molecules, such as amino silane coupling agents, have been widely used for the chemical introduction of the functional group on the surfaces of oxygenated carbon electrodes including diamond electrodes without any special apparatuses.[12,13] Since the CSCNF surface is known to be easily oxidized,[5,7] we herein report the electrochemical properties of CSCNFs chemically functionalized with amino groups using 3-aminopropyltriethoxysilane (APTES). We investigated electrochemical responses for the obtained NH_2-CSCNF electrode to two redox species, potassium ferricyanide ($K_3[Fe(CN)_6]$) and iron(II) sulfate ($FeSO_4$), which have been widely used for the characterization of the carbon electrode in the electrochemistry field. We also examined the prevention of protein adsorption at the NH_2-CSCNF surface for its application to bio-electroanalytical chemistry.

2. Experimental Procedure

2.1 Preparation of NH_2-CSCNF electrodes

A fluorine-doped tin-oxide (FTO, 10 Ω/□)-coated glass plate (Nippon Sheet Glass Co., Ltd., ø ~ 0.4 cm) was treated with a 1.0 M sodium hydroxide aqueous solution for 4 h to provide a negatively charged surface, followed by further treatment with a 2.5% acetic acid aqueous solution containing 2.5% APTES (Tokyo Chem. Ind. Co., Inc., Japan) for 4 h. After drying in an electric oven at 80 °C for 1 h, an aliquot of *N*,*N*-dimethylformamide (DMF) dispersion of CSCNF (Vision Development Co., Ltd., Japan) at 1.0 mg mL^{-1} was cast onto the APTES-modified FTO glass plate (ca. 40 μg cm^{-2}). Afterwards, the electrode was dried at room temperature and then stored in the electric oven at 80 °C for 15 min to completely remove DMF.

The surface of the obtained CSCNF electrode was further treated for 1 min with a vacuum oxygen plasma apparatus YHS-G200 (SAKIGAKE-Semiconductor Co., Ltd., Japan) at the oxygen flow ratio of 70 NL min^{-1} to introduce oxygen-containing functional groups. To obtain the NH_2-CSCNF electrode, the oxygen plasma-treated CSCNF (O_2-CSCNF) electrode was then immersed in the 2.5% acetic acid aqueous solution containing 2.5% APTES for 12 h, followed by drying in the electric oven at 80 °C for 1 h.

2.2 Evaluation of NH_2-CSCNF electrodes

The physical properties of bare CSCNFs, O_2-CSCNFs, and NH_2-CSCNFs at the FTO surface were evaluated by scanning electron microscopy (SEM, S-4800, Hitachi High-Tech Co., Japan), X-ray photoelectron spectroscopy (XPS, PHI5000, ULVAC-PHI, Inc.), and Raman spectroscopy (NRS-3300, JASCO Corp., Japan). The water contact angles of those CSCNF electrodes were measured using an optical microscope equipped for contact angle measurements.

Electrochemical measurements were performed using a potentiostat SP150 (Bio-Logic Science Instruments Ltd.). A three-electrode system was employed in the present work. Prepared electrodes were working electrodes. A Ag|AgCl|KCl (sat., RE-1CP, BAS, Japan) and a coiled platinum wire were the reference and counter electrodes, respectively. The electrochemical properties of the obtained electrodes were evaluated in a Briton Robinson buffer (BRB) containing 1 mM $K_3[Fe(CN)_6]$ in the presence and absence of 100 mg mL^{-1} bovine serum albumin (BSA, Fujifilm Wako Pure Chem. Ind., Corp., Japan) and 0.1 M sulfuric acid (H_2SO_4) solution containing 1 mM $FeSO_4$ by cyclic voltammetry. The BRB was prepared by mixing phosphoric acid (40 mM), acetic acid (40 mM), and boric acid (40 mM) with sodium hydroxide to reach the desired pH 7.4.

3. Results and Discussion

3.1 Characterization of NH_2-CSCNF electrodes

We first examined the physical properties of bare CSCNF, O_2-CSCNF, and NH_2-CSCNF electrodes using SEM. Figure 1(a) shows the SEM images of the bare CSCNFs, O_2-CSCNFs, and NH_2-CSCNFs at the FTO glass plate. Those three types of CSCNF seemed to be similar without any significant destruction and conformational changes even after the irradiation of oxygen plasma and the modification of APTES. Additionally, the diameter of those CSCNFs was determined to be about 50 nm. However, the water contact angle observed at the NH_2-CSCNF surface (ca. 23.4°) was clearly smaller than that at the bare CSCNF surface (ca. 82.2°) and slightly larger than that at the O_2-CSCNF surface (ca. 12.0°), as shown in Fig. 1(b). The oxygen plasma treatment has been known to produce carbonyl groups mainly on both basal and edge sites of graphite.[14] Therefore, hydrophilicity at the CSCNF surface after oxygen plasma treatment increased. Note that the water contact angle was almost the same even though the CSCNF surface was treated with oxygen plasma for 2 min. On the other hand, the pKa value for the amino group in APTES is known to be 9.6[15] and smaller than that for the carbonyl group (ca. 24–29),[16] namely, protonation might easily take place at the O_2-CSCNF surface in comparison with the NH_2-CSCNF surface. Thus, the pKa value likely contributed to the difference in water contact angle between NH_2-CSCNFs and O_2-CSCNFs. In addition, as distilled water generally shows a near-neutral pH, the NH_2-CSCNF surface should positively be charged. To verify this, the atomic oxygen-to-carbon (O/C) and nitrogen-to-carbon (N/C) ratios for the surfaces of the CSCNF samples were examined by XPS. The O/C ratio increased from 7% for bare CSCNF to 17% for O_2-CSCNF after the oxygen plasma treatment and then

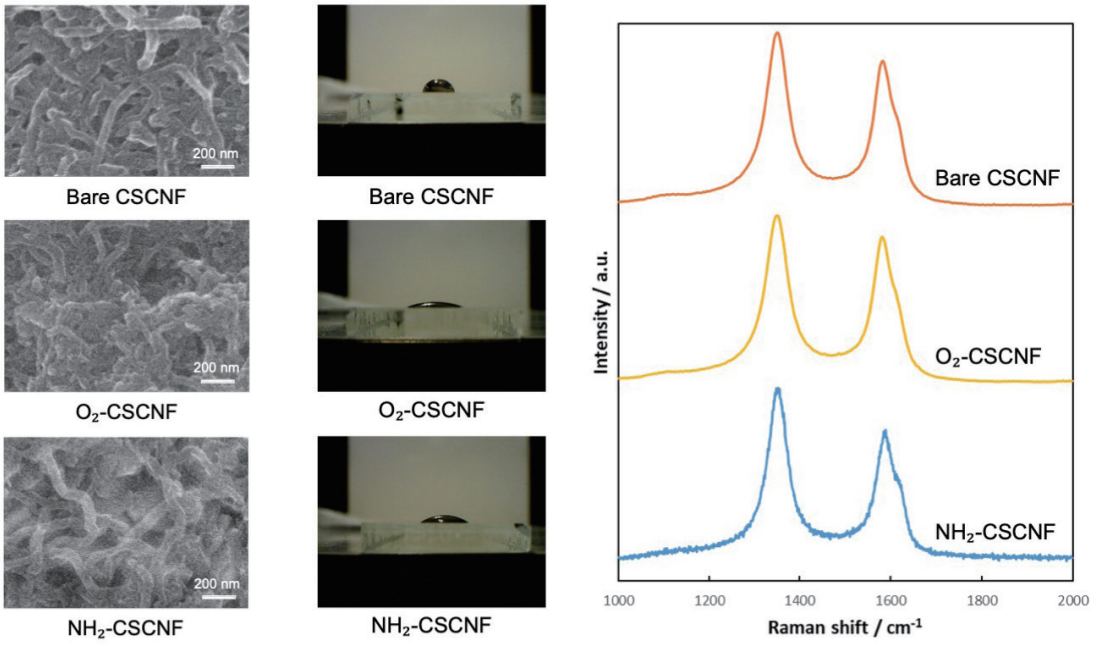

(a) (b) (c)

Fig. 1. (Color online) (a) SEM images of bare CSCNF, O_2-CSCNF, and NH_2-CSCNF electrodes. (b) Micrographs of 3 μL of water droplets on bare CSCNF, O_2-CSCNF, and NH_2-CSCNF electrode surfaces. (c) Raman spectra of bare CSCNF and O_2-CSCNF.

decreased to 14% for NH_2-CSCNF probably owing to the modification of APTES. This result may be reasonable, but almost no difference was observed for the N/C ratio among the three samples (~3%). The reason for this is unclear. Only a small amount of amino groups might be introduced to the CSCNF surface.

We also verified the structure of CSCNFs before and after the irradiation of oxygen plasma by Raman spectroscopy. As shown in Fig. 1(c), two strong Raman bands were observed at ~1350 and ~1580 cm^{-1} typically called the *D*- and *G*-bands, respectively. It has been known that the *D*-band corresponds to carbon atoms adjacent to a defect or a graphene edge, whereas the *G*-band is associated with a well-ordered graphitic framework.[17] A shoulder peak called *D*'-band, which arises from the edge plane of graphite,[18] also appeared at ~1615 cm^{-1}. This result certainly indicates that CSCNFs possess edge sites of graphene. According to the previous report, the relative intensity ratio of the *D*- and *G*-band peaks (I_D/I_G ratio) is often employed for the characterization of sp^2 carbon nanomaterials to estimate defects in their graphite structure.[19] On the basis of Fig. 1(c), the I_D/I_G ratio for O_2-CSCNF was determined to be about 1.14, which was slightly smaller than that for bare CSCNF (ca. 1.20). This result might suggest that peroxides or linkages forming between graphene sheets cause the carbon ends to become capped with the graphene sheets.[11] Thus, no significant severe damage was observed, even if the CSCNF surface was treated with oxygen plasma in this work. The I_D/I_G ratio for NH_2-CSCNF was also determined to be about 1.32, which was slightly larger than those for bare CSCNF (ca. 1.20) and O_2-CSCNF (ca. 1.14) owing to the presence of APTES. This result agreed well with the previous report.[20]

3.2 Electrochemical behavior of redox species

We next examined the electrochemical behavior of the two selected redox species. One is $[Fe(CN)_6]^{3-/4-}$, the redox behavior of which has been extensively studied in the electrochemistry field and widely used for the characterization of electrodes.[21] The other is $Fe^{2+/3+}$, the electron transfer kinetics of which has been known to be strongly sensitive to functional groups at the carbon surface.[22]

Figures 2(a) and 2(b) show cyclic voltammograms (CVs) in an air-saturated BRB containing 1 mM $[Fe(CN)_6]^{3-/4-}$ at the scan rate of 750 mV s^{-1} and an air-saturated 0.1 M H_2SO_4 aqueous solution containing 1 mM $FeSO_4$ at the scan rate of 300 mV s^{-1}. For $[Fe(CN)_6]^{3-/4-}$, there seemed a small difference in peak-to-peak potential separation (ΔE_P) among the bare CSCNF (ca. 86.3 mV), O_2-CSCNF (ca. 92.2 mV), and NH_2-CSCNF electrodes (ca. 86.2 mV). In addition, both anodic and cathodic peak currents for the three electrodes increased linearly with the square root of the scan rate below at least 1.0 V s^{-1}, indicating that the redox reaction is the diffusion-controlled process [Fig. 2(c)]. In this context, the apparent electroactive surface area in contact with the electrolyte solution was roughly estimated to be about 0.11, 0.12, and 0.12 cm^2 for the bare CSCNF, O_2-CSCNF, and NH_2-CSCNF on the FTO surface with a diameter of 0.4 cm, respectively, on the basis of the following Randles–Sevicik equation:

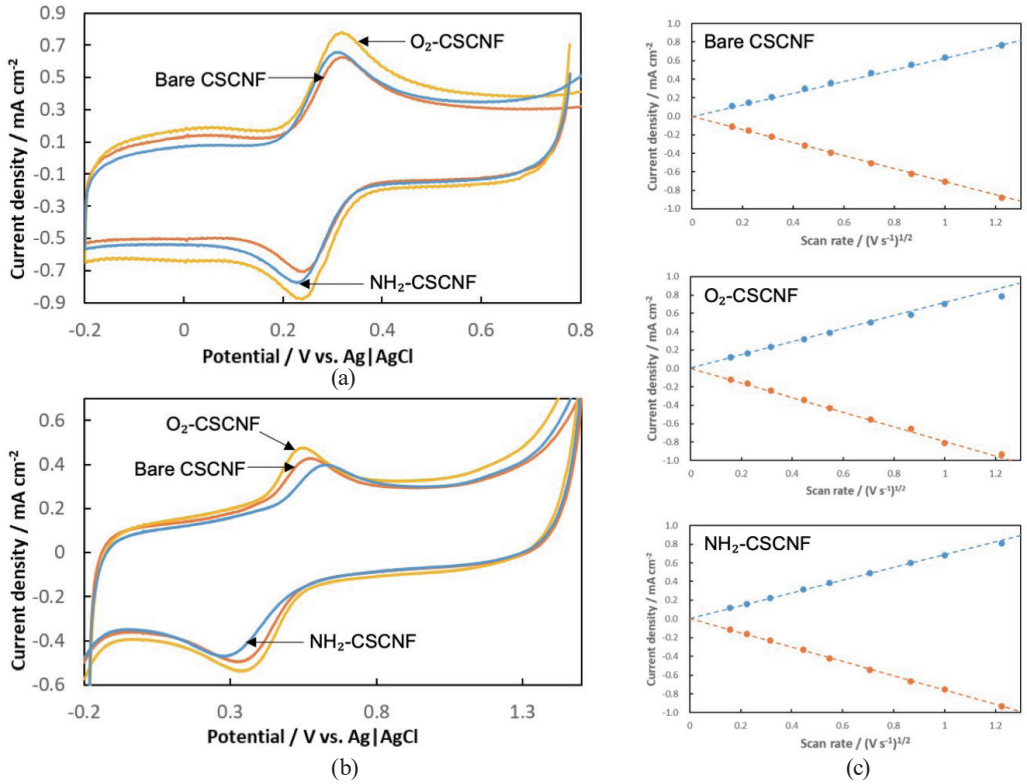

Fig. 2. (Color online) CVs of (a) 1 mM $[Fe(CN)_6]^{3-/4-}$ in the BRB and (b) 1 mM $Fe^{2+/3+}$ in the 0.1 M H_2SO_4 aqueous solution on bare CSCNF, O_2-CSCNF, and NH_2-CSCNF electrodes. Scan rates are (a) 750 and (b) 300 mV s^{-1}. (c) Dependences of anodic and cathodic peak currents on the square root of the scan rate at bare CSCNF, O_2-CSCNF, and NH_2-CSCNF electrodes in BRB containing 1 mM $[Fe(CN)_6]^{3-/4-}$.

$$I_P = 2.69 \times 10^5 AD^{1/2} n^{3/2} \nu^{1/2} C, \tag{1}$$

where I_P is the peak current for cyclic voltammetry, A is the electroactive surface area, D is the diffusion coefficient of $[Fe(CN)_6]^{3-/4-}$ as the redox probe to be 7.4×10^{-6} cm^2 s^{-1},[23] n is the number of electrons participating in the redox reaction (1 in the present case), ν is the scan rate, and C corresponds to the concentration of the redox probe. As mentioned above, the obtained apparent electroactive surface areas of the three electrodes were almost the same. The fast kinetics obtained here may therefore be strongly attributed to the edge plane sites, which may facilitate the electron transfer, but not the functional groups. In contrast, for $Fe^{2+/3+}$, the ΔE_P value for NH_2-CSCNF (ca. 373 mV) was clearly larger than those for bare CSCNF (ca. 235 mV) and O_2-CSCNF (ca. 208 mV). This reflects that the electron transfer kinetics of $Fe^{2+/3+}$ is strongly sensitive to the carbon surface, as described above.

On the basis of the cyclic voltammetry measurements, we calculated an apparent heterogenous electron transfer rate constant k^0_{app} at the projected surface area. For this, we employed the method developed by Nicholson [Eq. (2)],[24] which is widely used for the determination of k^0_{app} based on a quasi-reversible electrochemical reaction controlled by diffusion.

$$\psi = k^0_{app} \left(\frac{\pi D n \nu F}{RT} \right)^{-1/2} \tag{2}$$

Here, ψ is the kinetic parameter, F is the Faraday constant, R is the gas constant, and T is the temperature. The ψ value is easily calculated using Eq. (3) proposed by Lavagnini *et al.*,[25] where the ΔE_P value obtained at each scan rate is assigned.

$$\psi = \left(0.6288 + 0.0021 \Delta E_P\right) / \left(1 - 0.017 \Delta E_P\right) \tag{3}$$

A plot of the ψ values against $(\pi DnvF/RT)^{-1/2}$ should therefore give a straight line of slope k^0_{app}. The k^0_{app} value was calculated to be about 3.3×10^{-2}, 2.8×10^{-2}, and 3.8×10^{-2} cm s^{-1} for the bare CSCNF, O_2-CSCNF, and NH_2-CSCNF electrodes, respectively. Compared with the k^0_{app} value for bare CSCNF, that for NH_2-CSCNF was slightly larger, whereas that for O_2-CSCNF was slightly smaller. This result suggests that cationic amino groups positively and anionic oxygen-containing functional groups negatively contribute to the electron transfer rate of $[Fe(CN)_6]^{3-/4-}$, which is the anionic molecule, owing to the electrostatic interaction and repulsion, respectively. This point may be reasonable because the electron transfer of $[Fe(CN)_6]^{3-/4-}$ is known to be decelerated at oxygenated edge-oriented pyrolytic graphite,[26] oxygen-terminated diamond,[27] and graphene oxide electrodes,[28] whereas it is accelerated at the APTES-modified multiwalled carbon nanotube[12] and APTES-modified diamond.[13] Similarly, the electron transfer of $[Fe(CN)_6]^{3-/4-}$ is also known to be accelerated at nitrogen-doped carbon film electrodes, which consist of sp^2- and sp^3-bonded carbons with a low amount

of nitrogen-containing graphite-like and pyridine-like bonding structures.[29,30] Therefore, amino groups at the carbon surface contribute to the electron transfer kinetics for redox species. However, from the results obtained here, the electron transfer kinetics for $[Fe(CN)_6]^{3-/4-}$ in the present work is controlled by mainly graphene edges and partially functional groups at the CSCNF surface, such as carbonyl and amino groups.

In the case of $Fe^{2+/3+}$, when the diffusion coefficient $D = 5.1 \times 10^{-6}$ cm^2 s^{-1},[31] the k^0_{app} value was determined to be about 1.3×10^{-3} for bare CSCNF, 2.0×10^{-3} for O_2-CSCNF, and 6.0×10^{-4} cm s^{-1} for NH_2-CSCNF. As expected, the opposite property to $[Fe(CN)_6]^{3-/4-}$ was observed here, namely, the largest k^0_{app} value was O_2-CSCNF, followed in order by bare CSCNF and NH_2-CSCNF. Therefore, cationic amino groups negatively and anionic oxygen-containing functional groups positively contribute to the electron transfer rate of $Fe^{2+/3+}$, which is known to usually undergo inner-sphere redox reactions.[21,22] Thus, the oxygen plasma-treated and amino-functionalized CSCNF surface would allow the selectivity of electrochemical reactions to be tuned.

3.3 Electrochemical behavior of $[Fe(CN)_6]^{3-/4-}$ in the presence of protein

Considering the application to bioanalytical sensors, anti-protein fouling at the electrode surface is one of the crucial issues to maintain the performance of electrodes, such as sensitivity. Niwa and his co-workers have reported that the adsorption of a protein such as BSA is suppressed at electron cyclotron resonance (ECR)-sputtered nanocarbon film electrodes, the surface of which is treated with water vapor or ammonia gas plasma.[32] The decrease in current ratio for $[Fe(CN)_6]^{3-/4-}$ in the presence of 100 mg mL^{-1} BSA was within 30% in comparison with that in the absence of BSA.[10] We therefore examined the electrochemical behavior of $[Fe(CN)_6]^{3-/4-}$ at the O_2-CSCNF and NH_2-CSCNF electrodes in the BRB containing 100 mg mL^{-1} BSA by cyclic voltammetry. At the NH_2-CSCNF electrode, the anodic and cathodic peak currents of $[Fe(CN)_6]^{3-/4-}$ in the presence of 100 mg mL^{-1} BSA decreased about 22%, compared with those in the absence of BSA at the scan rate of 100 mV s^{-1}. In addition, the ΔE_P value for the former was about 70.9 mV, which was slightly larger than that for the latter (ca. 65.4 mV). Unfortunately, the NH_2-CSCNF electrode surface might be unable to completely eliminate the effect of protein fouling. However, this value was similar to the previous report.[10] We also found that the ΔE_P value gradually increased as the BSA concentration increased probably owing to the effect of BSA in the electrolyte solution [Fig. 3(a)]. Additionally, ΔE_P increased with the scan rate. On the basis of the CVs, similarly, the k^0_{app} value for $[Fe(CN)_6]^{3-/4-}$ in the presence of 100 mg mL^{-1} BSA ($k^0_{app,BSA}$) was determined to be about 1.5×10^{-2} for bare CSCNF, 1.8×10^{-2} for O_2-CSCNF, and 2.8×10^{-2} cm s^{-1} for NH_2-CSCNF. Note that although the viscosity of the electrolyte likely increased owing to the presence of BSA, such an effect was ignored in the calculation here. The obtained values were slightly smaller than those in the absence of BSA. Since $k^0_{app,BSA}$ depends on ΔE_P, as described above, such a decrease in $k^0_{app,BSA}$ would be based on the BSA adsorption partially.

We also evaluated the apparent heterogenous electron transfer rate constant ratio, $k^0_{app,BSA}/k^0_{app}$ As shown in Fig. 3(b), the $k^0_{app,BSA}/k^0_{app}$ value for the bare glassy carbon (GC) electrode, which is

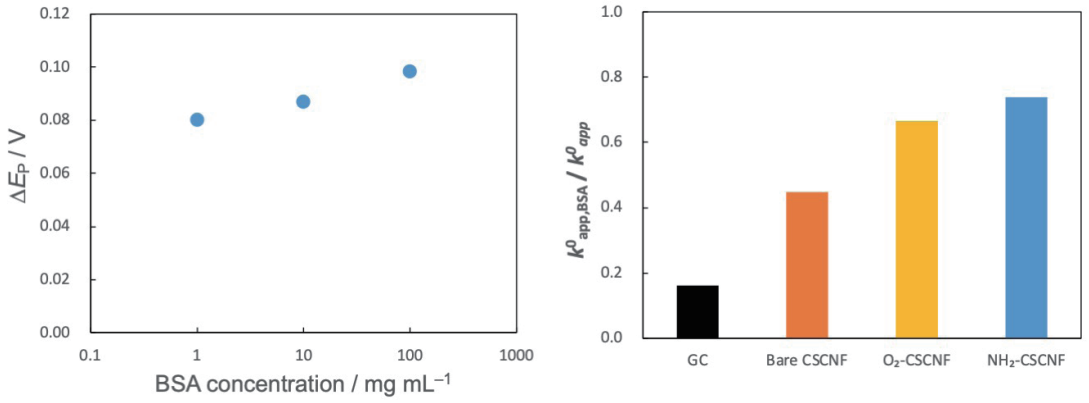

(a) (b)

Fig. 3. (Color online) (a) ΔE_P values of 1 mM $[Fe(CN)_6]^{3-/4-}$ at the NH_2-CSCNF electrode in BRB at the scan rate of 500 mV s^{-1}. (b) Comparison of $k^0_{app,BSA}/k^0_{app}$ ratio for $[Fe(CN)_6]^{3-/4-}$ in the presence and absence of 100 mg mL^{-1} BSA at GC, bare CSCNF, O_2-CSCNF, and NH_2-CSCNF electrodes.

widely used in the electrochemistry field, was about 0.16 owing to significant BSA adsorption. Such a blocking effect agreed well with the previous report.[33] The present O_2-CSCNF and NH_2-CSCNF electrodes cannot eliminate the BSA adsorption completely, but the $k^0_{app,BSA}/k^0_{app}$ values for those electrodes were much larger than that for the GC electrode. This result is reasonable because a highly hydrophilic surface at the electrode surface has been known to suppress protein fouling.[33] Incidentally, $k^0_{app,BSA}/k^0_{app}$ was slightly larger for NH_2-CSCNF than for O_2-CSCNF. As the isoelectric point for BSA is known to be 4.9, BSA should be negatively charged in the BRB (pH 7.4). If this holds, the BSA adsorption should easily take place at the positively charged NH_2-CSCNF surface owing to the electrostatic interaction rather than the negatively charged O_2-CSCNF surface. The factors for significant anti-BSA fouling might be not only the hydrophilicity and surface charge but also the surface roughness and morphology. This point is still unclear and one of the research topics in the future.

4. Conclusions

The electrochemical properties of NH_2-CSCNFs were investigated to explore their applicability as electrode materials. The kinetics of $[Fe(CN)_6]^{3-/4-}$ and $Fe^{2+/3+}$ is tunable with the NH_2-CSCNF surface. In addition, protein adsorption was suppressed owing to the hydrophilic and amino-functionalized surface. These factors are therefore subject to optimization in different applications, such as biosensing and other electrochemical devices.

Acknowledgments

We are very grateful to Prof. Kohei Shiraishi and Mr. Seiryu Hirao (Kindai University) for their help with the water contact angle measurement. This work was supported by Furukawa Technology Foundation.

References

1 X. Jia, J. Campos-Delgado, M. Terrones, V. Meunier, and M. S. Dresselhaus: Nanoscale **3** (2011) 86. https://doi.org/10.1039/C0NR00600A
2 R. W. Wightman, M. R. Deakin, P. M. Kovach, W. G. Kuhr, and K. J. Stutts: J. Electrochemical. Soc. **131** (1984) 1578. https://doi.org/10.1149/1.2115913
3 A. Ambrosi, A. Bonanni, and M. Pumera: Nanoscale **3** (2011) 2256. https://doi.org/10.1039/C1NR10136F
4 K. Komori, T. Tatsuma, and Y. Sakai: Langmuir **32** (2016) 9163. https://doi.org/10.1021/acs.langmuir.6b02407
5 S. Ko, Y. Takahashi, H. Fujita, T. Tatsuma, A. Sakoda, and K. Komori: RSC Adv. **2** (2012) 1444. https://doi.org/10.1039/C1RA00649E
6 K. Komori, Y. Komatsu, M. Nakane, and Y. Sakai: Bioelectrochemistry **138** (2021) 107719. https://doi.org/10.1016/j.bioelechem.2020.107719
7 S. Ko, T. Tatsuma, A. Sakoda, Y. Sakai, and K. Komori: Phys. Chem. Chem. Phys. **16** (2014) 12209. https://doi.org/10.1039/C4CP01278J
8 K. Komori, J. Huang, N. Mizushima, S. Ko, T. Tatsuma, and Y. Sakai: Phys. Chem. Chem. Phys. **19** (2017) 27795. https://doi.org/10.1039/C7CP04823H
9 M. Ardhaoui, M. Zheng, J. Pulpytel, D. Dowling, C. Jolivalt, and F. A. Khonsari: Bioelectrochemistry **91** (2013) 52. https://doi.org/10.1016/j.bioelechem.2012.12.005
10 S. Ohta, S. Shiba, T. Yajima, T. Kamata, D. Kato, and O. Niwa: J. Photopolym. Sci. Technol. **32** (2019) 523. https://doi.org/10.2494/photopolymer.32.523
11 K. Komori, S. Takumi, K. Kato, K. Matsumoto, K. Shiraishi, H. Kimura, and K. Takada: J. Electroanal. Chem. **943** (2023) 117621. https://doi.org/10.1016/j.jelechem.2023.117621
12 J. H. T. Luong, S. Hrapovic, D. Wang, F. Bensebaa, and B. Simard: Electroanalysis **16** (2004) 132. https://doi.org/10.1002/elan.200403113
13 H. Notsu, T. Fukazawa, T. Tatsuma, D. A. Tryk, and A. Fujishima: Electrochem. Solid-State Lett. **4** (2001) H1. https://doi.org/10.1149/1.1346556
14 M. Nakahara and Y. Sanada: J. Mater. Sci. **28** (1993) 1327. https://doi.org/10.1007/BF01191973
15 M. Valtiner, X. Banquy, K. Kristiansen, G. W. Greene, and J. N. Israelachvili: Langmuir **28** (2012) 13080. https://doi.org/10.1021/la3018216
16 S. Charvet, M. Médebielle, and J. C. Vantourout: J. Org. Chem. **87** (2022) 5690. https://doi.org/10.1021/acs.joc.2c00054
17 A. C. Ferrari, J. C. Meyer, V. Scardaci, C. Casiraghi, M. Lazzeri, F. Mauri, S. Picanec, D. Jiang, K. S. Novoselvo, S. Roth, A. K. Geim: Phys. Rev. Lett. **97** (2006) 187401. https://doi.org/10.1103/PhysRevLett.97.187401
18 L. Y. Jang, H. Ogata, K. C. Park, S. H. Lee, J. S. Park, Y. C. Jung, Y. J. Kim, Y. A. Kim, and M. Endo: J. Phys. Chem. Lett. **1** (2010) 2099. https://doi.org/10.1021/jz1006498
19 M. A. Pimenta, G. Dresselhaus, M. S. Dresselhaus, L. G. Cançado, A. Jorio, and R. Saito: Phys. Chem. Chem. Phys. **9** (2007) 1276. https://doi.org/10.1039/B613962K
20 L. Silvestro, A. S. Ruviaro, P. R. de Matos, F. Pelisser, D. Z. Meazlira, and P. J. P. Gleize: Constr. Build. Mater. **311** (2021) 125358. https://doi.org/10.1016/j.conbuildmat.2021.125358
21 P. Chen and R. L. McCreery: Anal. Chem. **68** (1996) 3958. https://doi.org/10.1021/ac960492r
22 P. Chen, M. A. Fryling, and R. L. McCreery: Anal. Chem. **67** (1995) 3115. https://doi.org/10.1021/ac00114a004
23 G. Gerhardt and R. L. Adams: Anal. Chem. **54** (1982) 2618. https://doi.org/10.1021/ac00251a054
24 R. S. Nicholson: Anal. Chem. **37** (1965) 1351. https://doi.org/10.1021/ac60230a016
25 I. Lavagnini, R. Antiochia, and F. Magno: Electroanalysis **16** (2004) 505. https://doi.org/10.1002/elan.200302851
26 X. Ji, C. E. Banks, A. Crossley, and R. G. Compton: ChemPhysChem **7** (2006) 1337. https://doi.org/10.1002/cphc.200600098
27 I. Yagi, H. Notsu, T. Kondo, D. A. Tryk, and A. Fujishima: J. Electroanal. Chem. **473** (1999) 173. https://doi.org/10.1016/S0022-0728(99)00027-3
28 A. Bonanni, A. Ambrosi, and M. Pumera: Chem. Eur. J. **18** (2012) 4541. https://doi.org/10.1002/chem.201104003
29 X. Yang, L. Haubold, G. DeVino, and G. M. Swain: Anal. Chem. **84** (2012) 6240. https://doi.org/10.1021/ac301124r
30 T. Kamata, D. Kato, S. Hirono, and O. Niwa: Anal. Chem. **85** (2013) 9845. https://doi.org/10.1021/ac402385q
31 C. Barbeco, J. J. Silber, and L. Sereno: J. Electroanal. Chem. Interfacial Electrochem. **248** (1988) 321. https://doi.org/10.1016/0022-0728(88)85093-9
32 Q. Xue, D. Kato, T. Kamata, S. Umemura, S. Hirono, and O. Niwa: Jpn. J. Appl. Phys. **51** (2012) 090124. http://dx.doi.org/10.1143/JJAP.51.090124
33 B. Guo, J.-I. Anzai, and T. Osa: Chem. Pharm. Bull. **44** (1996) 860. https://doi.org/10.1248/cpb.44.860